Journal of Anatomy

J. Anat. (2018) 233, pp679–684 doi: 10.1111/joa.12869

A radio-anatomical correlation study of the cisterna chyli

Yohann Renard,[1,2,3] Louis de Mestier,[4] Clémence Balaj,[1] Jean-Michel Arnoux,[1] Marc Labrousse,[2] Gabriela Hossu[3,5] and Manuela Perez[1,3]

[1]*Faculty of Medicine and University Hospital, Department of Anatomy, University of Lorraine, Nancy, France*
[2]*Faculty of Medicine and University Hospital, Department of Anatomy, University of Champagne-Ardenne, Reims, France*
[3]*IADI, INSERM 1254 University of Lorraine, Nancy, France*
[4]*Department of Pancreatology-Gastroenterology, Beaujon Hospital (APHP) and Paris 7 University, Clichy, France*
[5]*INSERM CIT1433, CIC-IT, University Hospital of Nancy, Nancy, France*

Abstract

Surgical laparoscopic procedures in the retroperitoneal and supramesocolic spaces are increasingly frequent. There is a high risk of iatrogenic intraoperative injury of the retroperitoneal lymphatic structures during these procedures. A precise understanding of the anatomy of the thoracic duct (TD) and the cisterna chyli (CC) is essential for safe surgical procedures in this area. However, routine imaging procedures rarely and often incorrectly visualize the CC. The objective of this study was to evaluate the feasibility of a retrograde injection of the TD to fill the CC with a contrast agent in 16 human cadavers. Both magnetic resonance lymphography (MRI) and computed tomography (CT) studies could be performed on the same anatomical specimen, using a contrast medium which hardened, allowing gross dissection. MRI and CT detectability were evaluated, and imaging results were compared with the anatomical dissection. The CC of 12/16 cadavers were successfully injected, and four were unsuccessful due to technical difficulties, showing the effectiveness of the method. This technique can improve understanding of the anatomy of the TD and CC and provides an original option to study the complex anatomy of these structures by correlating precise cadaveric dissections with cross-sectional imaging.

Key words: cisterna chyli; lymphatic capillaries; thoracic duct.

Introduction

The cisterna chyli (CC) and the emergence of the thoracic duct (TD) are the major lymphatic structures in the retroperitoneal and supramesocolic spaces (Pinto et al. 2004). These structures collect the lymphatic fluid from the minor lymphatic vessels that originate from all the abdominal organs (Pinto et al. 2004; Hematti & Mehran, 2011). Normally, the CC is located on the right, behind and very close to the abdominal aorta, on the anterior surface of the first or second lumbar vertebra (Akcali et al. 2006) and adjacent to the right crus of the diaphragm (Erden et al. 2005; Loukas et al. 2007). With the development and increase of surgical laparoscopic procedures around these areas, a clear understanding of the anatomy of these main abdominal lymphatic structures is essential to prevent intraoperative injuries to the CC (Akcali et al. 2006; Loukas et al. 2007) and subsequent chyle leakage (Weniger et al. 2016).

The CC has been extensively studied by cadaveric dissection, lymphangiography, cross-sectional imaging, computed tomography (CT) and magnetic resonance lymphography (MRI; Pinto et al. 2004; Akcali et al. 2006; Johnson & Seiler, 2006; Loukas et al. 2007), and numerous variations have been described (Pinto et al. 2004). However, to the best of our knowledge, there have been no studies evaluating the anatomical correlation between the features of the CC on CT and MRI and the real anatomy of the CC.

The aims of this study were to evaluate the feasibility of a retrograde injection of the CC through the TD in human cadavers and to investigate the value of the contrast dye mixture to compare the appearance of the lymphatic structures on MRI and CT with the true cadaveric anatomy. This method, combining cadaveric dissection and imaging of lymphatic vessels, should improve the understanding of complex anatomic structures, which are difficult to discriminate on routine imaging.

Correspondence
Yohann Renard, Faculty of Medicine and University Hospital, Department of Anatomy, University of Champagne-Ardenne, Reims, France, Rue Cognacq-Jay, 51092 Reims Cedex, France.
T: + 33 32 6787094; E: yrenard@chu-reims.fr

All authors contributed equally to this work.

Accepted for publication *11 July 2018*
Article published online *12 August 2018*

Materials and methods

Sixteen fresh human cadavers were used for this study, seven females and nine males, mean age 76.9 years (range 63–93). Cadavers had been donated to the Department of Anatomy, Faculty of Medicine and University Hospital, Lorraine University, for anatomical education and research. All the ethical rules concerning work on cadaveric material in our institution (Law 94-653 of July 29, 1994 relative to the respect of the human body) were followed for this study. First, each cadaver was dissected. Then, subjects were placed in the supine position and the right chest wall was opened along a medial axillary line from the clavicle to the diaphragmatic attachments. The chest flap was removed or laid back (Fig. 1). The TD was searched for on the right side of the lower thoracic segment, between the thoracic aorta and the azygos vein. Once the TD had been identified and dissected, it was ligatured superiorly and catheterized with a 70-mm button cannula (Meiser Medical®, Neuenstein, Germany) (Fig. 2A). An injection of green latex mixed with barite at a concentration of 10% and gadobutrol at a concentration of 3 mL/L was performed as reported in the literature (Fig. 2B; Renard et al. 2017). Because of the fragility of the lymphatic vessels, the injection was performed slowly and carefully with a 5-mL syringe (BD Medical®, Le Pont-de-Claix, France). Filling of the CC and its trunks was stopped when the pressure of injection became too high. This injected volume was then noted.

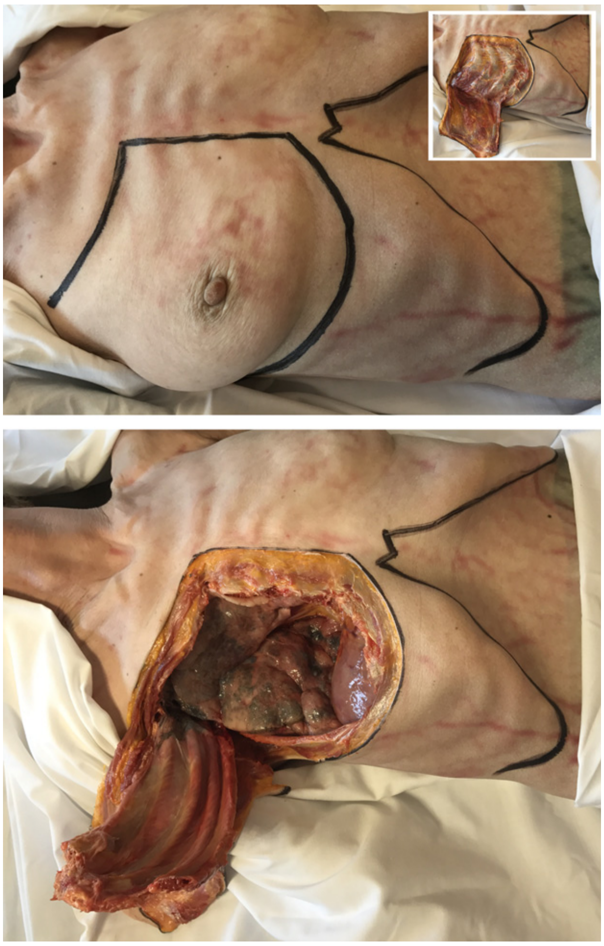

Fig. 1 Chest approach of the thoracic duct.

MR examinations were performed on a 3T MR scan (Signa HDxt; GE Healthcare, Milwaukee, WI, USA) with an 8-channel surface phased-array coil (8US TORSOPA). A 3D Fast Spoiled Gradient Echo (FSPGR) sequence was obtained for all acquisitions: repetition time (TR) 8.5 ms; echo time (TE) around 3.6 ms; excitation, 4; matrix, 179×256; field of view, 300 mm; slice thickness 0.8 mm with 0.4 mm gap; the resulting resolution was 0.6×0.6 mm.

CT-scan studies were performed using a 256-slice multidetector CT scanner (Revolution, General Electric Healthcare, USA) with helical mode (1.0 mm collimation, 120 kV, 110 mA, pitch 2, slice thickness 0.62 mm, matrix 512×512 and a field of view of 275×275 mm^2).

All post-processing was performed with the 3D maximum intensity projection technique with Object Research System (ORS) Visual software version 1.5 (Montreal, Canada).

After imaging, the abdomen was opened by large vertical incisions from the pubis to the xiphoid process and transversal incisions joining the two flanks. The injected CC was dissected, exposed and measured, and its precise location in relation to the main vessels was noted, as well as the existence of the injected collateral trunk.

Results

The characteristics of the anatomical subjects and the results of injections are reported in Table 1. Catheterization of the TD was not possible in two cases (12%) because it could not be found or was too thin. Thus, no scans or dissections were performed in these two subjects. The mean injected volume in the 14 remaining subjects was 14.5 mL (range 8–25). In four cases injection of the contrast mixture led to leakage outside of the lymphatic structures in the upper part of the retroperitoneal space, as observed on MRI and CT; however, a complete radiological and anatomical study of the CC was still possible in two of them. Finally, 12 subjects underwent the complete MRI and CT protocol, followed by anatomical dissection. The anatomical details studied on MRI and CT in these subjects could be compared precisely with anatomical findings after dissection. Details of the different afferent trunks forming the CC were specifically visualized. Figures 3–6 show the highly comparable anatomical findings between radiological and anatomical studies. The CC of three subjects (25%) originated from two afferent trunks (Fig. 5), six (50%) from three afferent trunks (Figs 3 and 4) and three (25%) from four afferent trunks (Fig. 6). There was no dilation in the site of the TD origin in five subjects (41%, Fig. 6).

Discussion

Direct surgical trauma of the CC and its main afferent ducts is of growing importance following abdominal surgery because of the increase in laparoscopic abdominal procedures (Weniger et al. 2016). CC injuries have been reported after anterior spinal procedures (Akcali et al. 2006), blunt abdominal trauma (Haan et al. 2007), laparoscopic

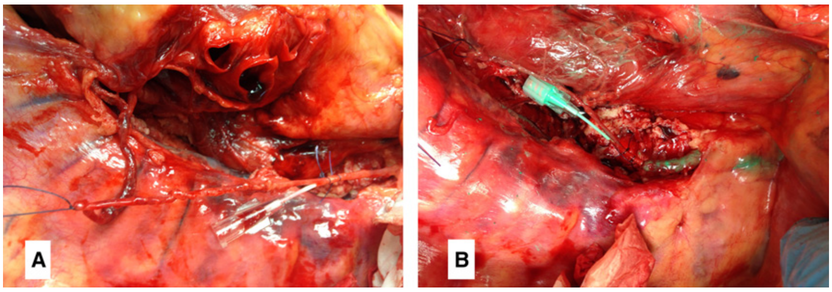

Fig. 2 (A) Catheterization of the thoracic duct. (B) Injection through the thoracic duct.

Table 1 Subject characteristics and injection results.

Subject	Gender	Age (years)	Injected volume (mL)	Leakage during injection	Complete study	Number of trunks	Initial dilation (cisterna)
1	Male	74	10	X			
2	Male	87	10		X	3	
3	Male	63	8.5	X			
4	Female	91	10.5		X	2	X
5	Male	67	9.5		X	4	
6	Female	86	9	X	X	4	X
7	Male	63	Failure				
8	Male	67	12		X	3	X
9	Female	88	8		X	3	
10	Female	82	15		X	3	
11	Male	93	Failure				
12	Male	68	20		X	3	X
13	Female	74	15	X	X	2	
14	Female	81	25		X	4	X
15	Female	76	15		X	3	X
16	Male	71	25		X	2	X

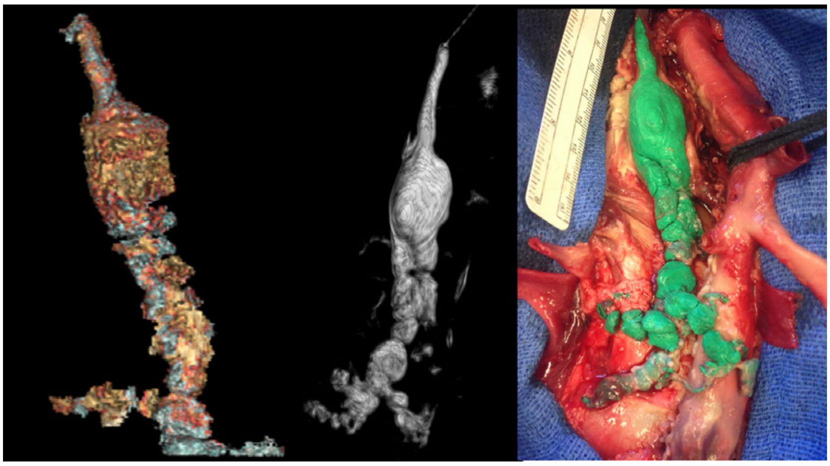

Fig. 3 MRI, CT and anatomical (from left to right) results of the cisterna chyli (CC) study in subject number 12. The CC originated from three afferent trunks.

cholecystectomy (Gogalniceanu et al. 2010), laparoscopic nephrectomy (Caumartin et al. 2005) as well as pelvic, colorectal, hepatic, pancreatic and gastric surgery with incidence rates varying from 1 to 11% (Weniger et al. 2016). CC injuries may cause chylous leakage, resulting in chylous ascites, usually leading to significant morbidity from

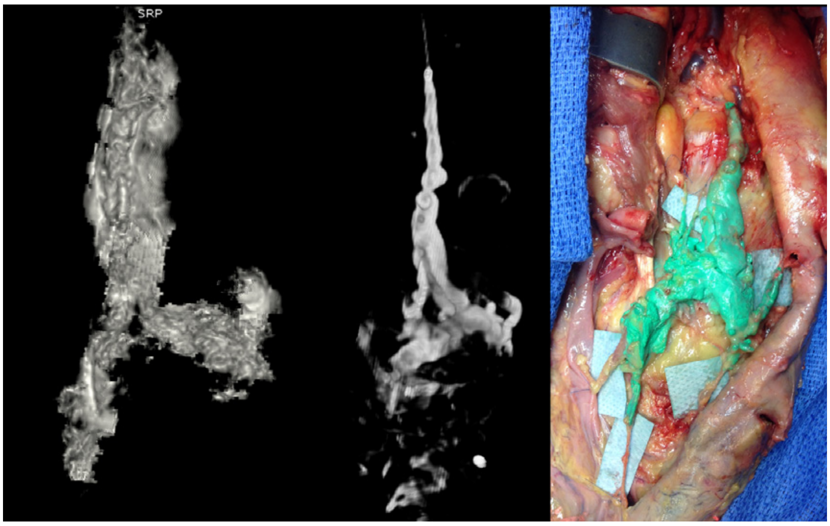

Fig. 4 MRI, CT-scan and anatomical (from left to right) results of the cisterna chyli (CC) study in subject number 15. The CC originated from three afferent trunks.

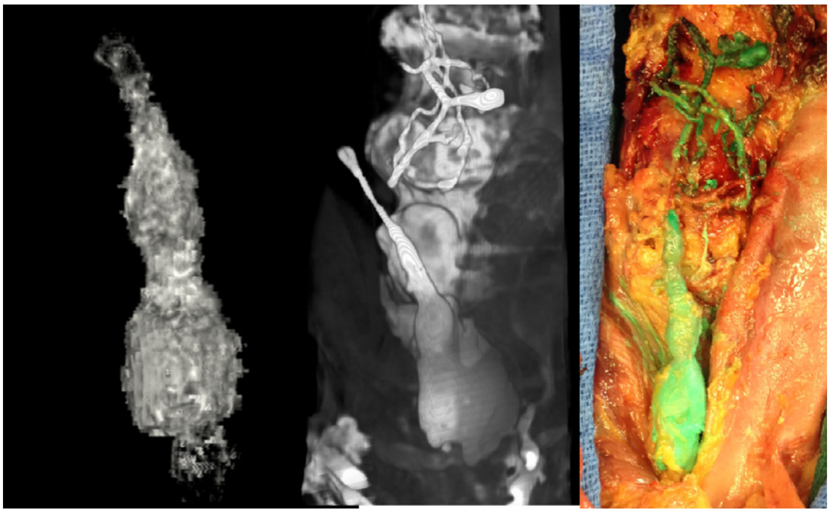

Fig. 5 MRI, CT-scan and anatomical (from left to right) results of the cisterna chyli (CC) study in subject number 16. The CC originated from two afferent trunks.

malnutrition, immunosuppression and septic complications (Akcali et al. 2006; Weniger et al. 2016). Thus, accurate knowledge of the CC and TD anatomies is needed. Furthermore, the prognostic importance of lymph-node status in patients with digestive cancers (Fink et al. 2016) and the high rate of regional lymph-node recurrence after cancer resection, even after extended lymphadenectomy (Riediger et al. 2009), have created an interest in anatomical knowledge of the abdominal lymphatic circulation (Borghi et al. 1998; Samra et al. 2008).

Lymphatic structures are extremely difficult to identify on routine imaging. Conventional lymphangiography has been the basis of lymphatic imaging and the CC was visualized in approximately 50% of those studies (Pinto et al. 2004). Although it involves invasive procedures and patient discomfort (Arrivé et al. 2007), lymphangiography is a valuable tool for the detection of 64–78% of lymphatic leakages (Lee et al. 2014). The normal CC is rarely visible on a routine CT-scan, even with intravenous contrast administration (1.7–16.1% of abdominal CT-scans) (Smith & Grigoropoulos, 2002; Feuerlein et al. 2009), probably because lymphatic capillaries are very thin and have very low contrast enhancement (Feuerlein et al. 2009; Kiyonaga et al. 2012). Furthermore, the appearance of the CC can mimic an enlarged retrocrural lymph node on abdominal CT and correct identification is quite difficult (Gollub & Castellino, 1996; Pinto et al. 2004; Feuerlein et al. 2009), unless it is specifically studied on thin-slice, multiplanar reconstructions (Kiyonaga et al. 2012). The CC is also difficult to differentiate from vascular structures or retrocrural lymph nodes on

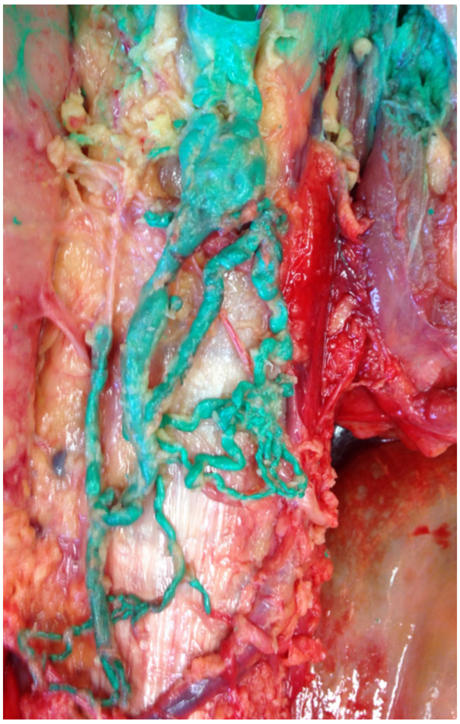

Fig. 6 Origin of the thoracic duct in subject number 16, without initial dilation and originating from four afferent trunks.

abdominal ultrasound (Tamsel et al. 2006; Wachsberg, 2006; Etienne et al. 2013). In patients with chyloabdomen or chylothorax, ultrasound has been described as a method to guide percutaneous embolization of the thoracic duct via the CC once it is opacified during lymphangiography (Hoffer et al. 2001; Syed et al. 2007; Lee et al. 2014). Standard abdominal MRI, generally including highly fluid-sensitive T2-weighted sequences, only identifies the CC in 15% of patients (Pinto et al. 2004). A specific MR protocol with thinner sections and fat suppression (heavily T2-weighted fast spin-echo) provides adequate evaluation of the abdominal and retroperitoneal lymphatic system (Arrivé et al. 2007). The origin of the TD was identified in 87%–96% of images with this sequence (Erden et al. 2005; Johnson & Seiler, 2006). Gadolinium injection helps differentiate the CC on delayed phase images from lymph nodes, the azygos vein or esophageal varices (Arrivé et al. 2007; Verma et al. 2007). In summary, the CC is difficult to visualize on routine *in vivo* imaging (Feuerlein et al. 2009; Kiyonaga et al. 2012), and ultrasound, conventional CT and MRI examinations are not useful in practice (Akcali et al. 2006).

The present study reports an original method to enhance contrast of the CC and TD on *ex vivo* MRI and CT. The common technique involving cannulation of the CC is usually performed percutaneously, following opacification of the CC with lipiodol, similar to the approach taken during TD embolization for the treatment of lymphatic leakage (Lee et al. 2014; Stecker & Fan, 2016). We report another technique including cannulation of the TD and retrograde injection of a contrast agent into the CC. This method is similar to the technique described by Mittleider et al. (2008) which involves direct access to the TD from the subclavian vein for TD embolization.

In our study, the injection was performed using green latex mixed with barite and gadobutrol as previously described (Renard et al. 2017). This made it possible to identify systematically the origin of the TD and CC, when it existed, on high resolution CT and MRI. Anatomical comparisons were also possible between the two imaging techniques.

Precise gross dissection of the injected CC was also possible with this technique after the imaging studies, since the green contrast agent hardened. Otherwise, it is extremely difficult to identify the CC during cadaveric dissection, with significant variations of results in the literature. Loukas et al. identified the CC in 83.3% of specimens in a study of 120 adult cadavers and Kubik et al. in 20% (14 of 70 dissections), whereas Propst-Proctor et al. (1983) only identified the CC in 1.2% (12 of 1000) patients during anterior spine surgery (Loukas et al. 2007; Propst-Proctor et al. 1983). Our technique allowed rapid identification and meticulous dissection of the lymphatic structures in all injected subjects as well as direct morphological comparisons between imaging findings and the precise anatomy of the TD and CC. The appearance of the CC on MRI, CT and after dissection was found to be exactly the same in the 12 anatomical injected subjects in the present study.

Although this was not our goal, we were able precisely to describe the anatomy of the CC with this technique, which was usually formed by the union of the right and left lumbar and the intestinal trunks (Pinto et al. 2004; Erden et al. 2005; Loukas et al. 2007). Many authors have described numerous variations including sacculations and considerable differences in the size and in shape of this structure and its afferent trunks (Pissas, 1984; Hirai et al. 2001a,b; Loukas et al. 2007; Mirilas & Skandalakis, 2010). Our study identified 3/12 TD origins formed by four trunks, corresponding to Types II and IV, and 9/12 TD formed by two or three trunks, corresponding to Types I and III, respectively, in the study by Loukas et al. (2007). However, these classifications do not provide details on the location of each trunk and their respective contribution to the formation of the CC, showing that this structure requires further study (Loukas et al. 2007). Larger series using our technique may help respond to these questions.

In conclusion, it is essential to combine the anatomical precision of cadaveric dissections with cross-sectional imaging. An understanding of the complex anatomy of the TD and CC could improve knowledge of structures that are difficult to identify on routine abdominal imaging such as the retroperitoneal lymphatic pathways. The present study confirms the feasibility of a retrograde injection of the CC through the TD in 12 cadavers. We also show that this mixture improves contrast enhancement on both MRI and CT, with excellent anatomical correlations with the real gross anatomy. The anatomical appearance of injected structures observed on MRI, CT and an anatomical cast after dissection were found to be highly similar.

Acknowledgements

The authors acknowledge the financial help of the FEDER, CPER program and the 'Région Lorraine', Mrs. Jocelyne Wuibout and Ms Dale Roche-Lebrec, editors of Medical English (PhD), for editing this manuscript.

Disclosure of interests

The authors have no conflict of interest to declare.

References

Akcali O, Kiray A, Ergur I, et al. (2006) Thoracic duct variations may complicate the anterior spine procedures. *Eur Spine J* **15**, 1347–1351.

Arrivé L, Azizi L, Lewin M, et al. (2007) MR lymphography of abdominal and retroperitoneal lymphatic vessels. *Am J Roentgenol* **189**, 1051–1058.

Borghi F, Gattolin A, Garbossa D, et al. (1998) Embryologic bases of extended radical resection in pancreatic cancer. *Arch Surg* **133**, 297–301.

Caumartin Y, Pouliot F, Sabbagh R, et al. (2005) Chylous ascites as a complication of laparoscopic donor nephrectomy. *Transpl Int* **18**, 1378–1381.

Erden A, Fitoz S, Yagmurlu B, et al. (2005) Abdominal confluence of lymph trunks: detectability and morphology on heavily T2-weighted images. *AJR Am J Roentgenol* **184**, 35–40.

Etienne AL, Cavrenne R, Gommeren K, et al. (2013) Ultrasonographic characteristics of the cisterna chyli in eight dogs and four cats. *Vet Radiol Ultrasound* **54**, 398–402.

Feuerlein S, Kreuzer G, Schmidt SA, et al. (2009) The cisterna chyli: prevalence, characteristics and predisposing factors. *Eur Radiol* **19**, 73–78.

Fink DM, Steele MM, Hollingsworth MA (2016) The lymphatic system and pancreatic cancer. *Cancer Lett* **381**, 217–236.

Gogalniceanu P, Purkayastha S, Spalding D, et al. (2010) Chyle leak following laparoscopic cholecystectomy: a rare complication. *Ann R Coll Surg Engl* **92**, e12–e14.

Gollub MJ, Castellino RA (1996) The cisterna chyli: a potential mimic of retrocrural lymphadenopathy on CT scans. *Radiology* **199**, 477–480.

Haan JM, Montgomery S, Novosel TJ, et al. (2007) Chyloperitoneum after blunt abdominal injury. *Am Surg* **73**, 811–813.

Hematti H, Mehran RJ (2011) Anatomy of the thoracic duct. *Thorac Surg Clin* **21**, 229–238, ix.

Hirai I, Murakami G, Kimura W, et al. (2001a) Long descending lymphatic pathway from the pancreaticoduodenal region to the para-aortic nodes: its laterality and topographical relationship with the celiac plexus. *Okajimas Folia Anat Jpn* **77**, 189–199.

Hirai I, Murakami G, Kimura W, et al. (2001b) Origin of the thoracic duct and pancreaticoduodenal lymphatic pathways to the para-aortic lymph nodes. *J Hepatobiliary Pancreat Surg* **8**, 441–448.

Hoffer EK, Bloch RD, Mulligan MS, et al. (2001) Treatment of chylothorax. *Am J Roentgenol* **176**, 1040–1042.

Johnson VS, Seiler G (2006) Magnetic resonance imaging appearance of the cisterna chyli. *Vet Radiol Ultrasound* **47**, 461–464.

Kiyonaga M, Mori H, Matsumoto S, et al. (2012) Thoracic duct and cisterna chyli: evaluation with multidetector row CT. *Br J Radiol* **85**, 1052–1058.

Kubik S (1995) Cardiovascular system. In: *Gray's Anatomy*. 38th edn (eds. Williams PL, Bannister LH, Berry MM), p. 1610. New York: Churchill Livingstone.

Lee EW, Shin JH, Ko HK, et al. (2014) Lymphangiography to treat postoperative lymphatic leakage: a technical review. *Korean J Radiol* **15**, 724–732.

Loukas M, Wartmann CT, Louis RG, et al. (2007) Cisterna chyli: a detailed anatomic investigation. *Clin Anat* **20**, 683–688.

Mirilas P, Skandalakis JE (2010) Surgical anatomy of the retroperitoneal spaces, Part III: Retroperitoneal blood vessels and lymphatics. *Am Surg* **76**, 139–144.

Mittleider D, Dykes TA, Cicuto KP, et al. (2008) Retrograde cannulation of the thoracic duct and embolization of the cisterna chyli in the treatment of chylous ascites. *J Vasc Interv Radiol* **19**, 285–290.

Pinto PS, Sirlin CB, Andrade-Barreto OA, et al. (2004) Cisterna chyli at routine abdominal MR imaging: a normal anatomic structure in the retrocrural space. *Radiographics* **24**, 809–817.

Pissas A (1984) Anatomoclinical and anatomosurgical essay on the lymphatic circulation of the pancreas. *Anat Clin* **6**, 255–280.

Propst-Proctor SL, Rinsky LA, Bleck EE (1983) The cisterna chyli in orthopaedic surgery. *Spine* **8**, 787–792.

Renard Y, Hossu G, Chen B, et al. (2017) A guide for effective anatomical vascularization studies: useful ex vivo methods for both CT and MRI imaging before dissection. *J Anat* **232**(1), 15–25.

Riediger H, Keck T, Wellner U, et al. (2009) The lymph node ratio is the strongest prognostic factor after resection of pancreatic cancer. *J Gastrointest Surg* **13**, 1337–1344.

Samra JS, Gananadha S, Hugh TJ (2008) Surgical management of carcinoma of the head of pancreas: extended lymphadenectomy or modified en bloc resection? *ANZ J Surg* **78**, 228–236.

Smith TR, Grigoropoulos J (2002) The cisterna chyli: incidence and characteristics on CT. *Clin Imaging* **26**, 18–22.

Stecker MS, Fan CM (2016) Lymphangiography for thoracic duct interventions. *Tech Vasc Interv Radiol* **19**, 277–285.

Syed LH, Georgiades CS, Hart VL (2007) Lymphangiography: a case study. *Semin Interv Radiol* **24**, 106–110.

Tamsel S, Ozbek SS, Sever A, et al. (2006) Unusually large cisterna chyli: US and MRI findings. *Abdom Imaging* **31**, 719–721.

Verma SK, Mitchell DG, Bergin D, et al. (2007) The cisterna chyli: enhancement on delayed phase MR images after intravenous administration of gadolinium chelate. *Radiology* **244**, 791–796.

Wachsberg RH (2006) Ultrasonography of the retrocrural region: normal and pathological findings. *Ultrasound Q* **22**, 281–290.

Weniger M, D'Haese JG, Angele MK, et al. (2016) Treatment options for chylous ascites after major abdominal surgery: a systematic review. *Am J Surg* **211**, 206–213.